Inorganica Chimica Acta xxx (2017) xxx–xxx

Contents lists available at ScienceDirect

Inorganica Chimica Acta

journal homepage: www.elsevier.com/locate/ica

Research paper

N-heterocyclic carbene complexes of palladium in oxygen atom transfer reactions involving the making and breaking of N-O bonds

Xiaochen Cai [a], Subhojit Majumdar [a], Leonardo F. Serafim [a], Manuel Temprado [b,*], Steven P. Nolan [c,*], Catherine S.J. Cazin [c,*], Burjor Captain [a,*], Carl D. Hoff [a,*]

[a] Department of Chemistry, University of Miami, Coral Gables, FL 33146, United States
[b] Department of Analytical Chemistry, Physical Chemistry and Chemical Engineering, Universidad de Alcalá, Madrid 28801, Spain
[c] Department of Inorganic and Physical Chemistry, Ghent University, Krijgslaan 281, S-3, Ghent 9000, Belgium

ARTICLE INFO

Article history:
Received 14 March 2017
Received in revised form 29 May 2017
Accepted 30 May 2017
Available online xxxx

ABSTRACT

Reaction of three equivalents of MesCNO (Mes = 2,4,6-trimethylphenyl) with one equivalent of [Pd(IPr)(P(p-tolyl)$_3$)] in toluene yields the solid complex [Pd(IPr)(NCMes)(κ^2-O–N=C-Mes(–N–C(=O)Mes))]. Three major steps are proposed to be involved in the reaction based on spectroscopic studies as well as literature precedents for related cycloadditions: i. oxidation of the coordinated phosphine ligand to phosphine oxide ii. oxygen atom transfer forming a C=O bond from the N–O bond of MesCNO, and iii. cycloaddition of a final MesCNO ligand to yield product.

Addition of two equivalents of ·NO at low temperature to the *in situ* generated peroxide complex [Pd(IPr)$_2$(η^2-O$_2$)] generates the N-bonded complex *trans*-[Pd(IPr)$_2$(NO$_2$)$_2$] in keeping with a literature precedent reported for similar complexes. Insight into the energetics of this reaction are probed by DFT calculations using the truncated ligand complex [Pd(IMe)$_2$]. The computed enthalpy of binding of two moles of ·NO$_2$ to form [Pd(IMe)$_2$(NO$_2$)$_2$] is −112 kcal/mol indicating that its preparation from [Pd(IMe)$_2$], N$_2$ and 2O$_2$ is thermodynamically favorable by −96 kcal/mol. Crystal structures of [Pd(IPr)(NCMes)(κ^2-O–N=C-Mes(–N–C(=O)Mes))] and *trans*-[Pd(IPr)$_2$(NO$_2$)$_2$] are reported.

1. Introduction

Cycloaddition reactions of nitrile oxides are a complex and important area of organic chemistry. They have been utilized in a wide range of situations, for example, Echegoyen and co-workers [1] have reported addition and removal of RCNO to a modified fullerene in a cycloaddition reaction illustrated in Eq. (1):

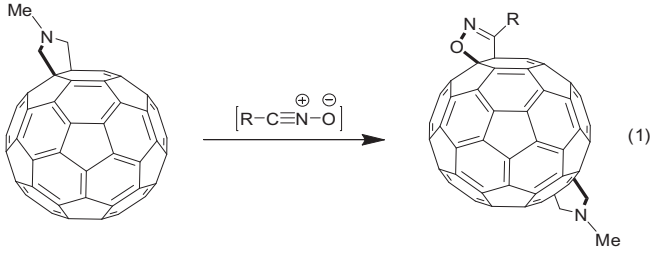

(1)

Due to the low N-O bond dissociation enthalpy (BDE) in ArCNO (≈54 kcal/mol) [2], oxygen atom transfer (OAT) can occur readily to an oxygen atom acceptor. In this context, Beck and coworkers [3] have reported a highly unusual P-arene bond cleavage reaction in conjunction with oxidation at P of the PPh$_3$ ligand to form a coordinated phosphine oxide in reaction of a series of nitrile oxides with zerovalent Pt phosphine complexes.

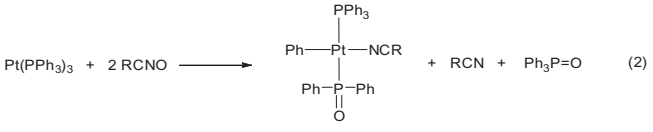

(2)

We have utilized MesCNO in kinetic and mechanistic studies [4] of cleavage of a range of N-O bonds in reactions such as the one shown in Eq. (3) for MesCNO:

$$(Ar(^tBu)N)_3V + MesCNO \rightarrow (Ar(^tBu)N)_3VO + MesCN \quad (3)$$

* Corresponding authors.
E-mail addresses: steven.nolan@ugent.be (S.P. Nolan), c.hoff@miami.edu (C.D. Hoff).

http://dx.doi.org/10.1016/j.ica.2017.05.069
0020-1693/

Due to the strong O=VL_3 bond in the product formed through Eq. (3), this reaction is exothermic by nearly 100 kcal/mol [4] and occurs rapidly even at low temperature. That is not surprising for early transition metal complexes which are known to have strong metal-oxo bonds.

This work was begun in attempts to see if OAT to coordinatively unsaturated low valent Pd complexes could occur as shown in Eq. (4):

$$Pd(L)_2 + MesCNO \rightarrow (L)_2Pd(NCMes)(O) \quad (4)$$

The reaction shown in Eq. (4) would produce a square planar d^8 complex of Pd(II) which would not have an empty d orbital on Pd for π bonding to lone pairs on O and thus would be predicted to be unstable due to the "oxo-wall" effect [5]. The "oxo-wall" concept applies to stable species and does not rule out formation of transient intermediates. Studies of CO_2 exchange with a labelled carbonate complex were proposed by Gould and coworkers [6] to involve generation of a Pt=O oxo complex intermediate as shown in Eq. (5):

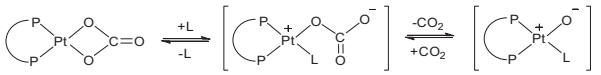

(5)

An analogous mechanism was proposed by Bohle and co-workers [7] in reaction of the hyponitrite complex shown in reaction (6):

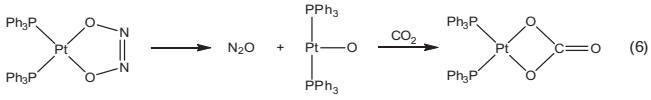

(6)

The resonance formulas for N≡N–O ↔ N=N=O and their nitrile oxide counterparts are formally equivalent R–C≡N–O ↔ R–C=N=O. The characteristic 1,3 dipolar addition reactions of the nitrile oxide, as illustrated in Eq. (1) also have inorganic metal based counterparts as elucidated in a number of detailed studies by Kukushkin and coworkers [8]. These types of cycloadditions also play a prominent role in oxidative reactions such as that shown in Eq. (7):

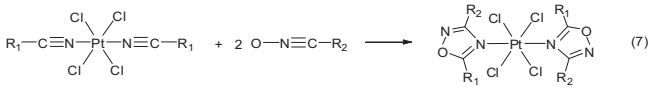
(7)

In this reaction, the metal serves to accelerate the cycloaddition process and the metal itself is not oxidized. However as shown in the work of Beck [3] in Eq. (2) OAT may also play a role culminating in oxidation of a bound phosphine ligand.

Related chemistry, and the only isolated late transition metal oxo complex reported to date has been reported by Milstein [9]. The higher energy OAT reagent peroxyacetone was used as shown in Eq. (8):

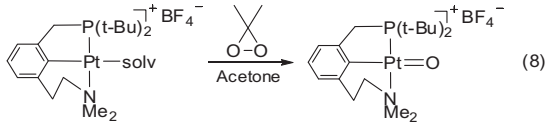

(8)

The Pt(IV) oxo complex is a d^6 ion and thus does not violate the "oxo-wall" axiom [5] related to the unstable nature of metal oxo complexes lacking an empty d-orbital to participate in π-acceptance of at least one of the oxide ion lone pairs. This complex undergoes oxidation of the coordinated phosphine of the pincer ligand as shown in Eq. (9):

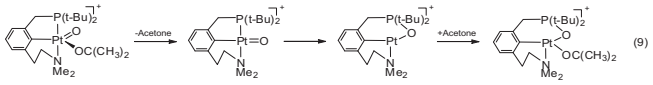

(9)

The facile OAT to the phosphine arm of the pincer ligand in Eq. (6) is similar to that observed by Beck and coworkers in Eq. (2). The Pt=O BDE in the Milstein complex can be estimated from reported computational data to be on the order of ≈30 kcal/mol.

Bergman and coworkers [10] investigated coupling of two equivalents of benzonitrile at the early transition metal Zr=O complex shown in Eq. (10):

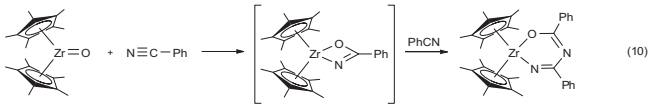

(10)

In principle, this reaction could be imagined to have begun with $ZrCp*_2$ and PhCNO which would be expected to undergo rapid OAT to form O-$ZrCp*_2$ and PhCN. The first step in (10) involves breaking the Zr=O bond and its transfer to the C atom of PhCN to form the chelating benzamide complex. In the second step of the reaction the highly basic N atom of the benzamido complex performs nucleophilic attack at the C atom of a second equivalent of benzonitrile to form the metallacyclic complex.

Recently, we have utilized MesCNO (N-O BDE of 54 kcal/mol) [2] to study the thermodynamics and kinetics of OAT reactions to PR_3, N-heterocyclic carbenes (NHC) and metal containing complexes [4,11]. The mechanism for oxidation of free phosphine ligands was proposed [11] to occur as shown in Scheme 1.

Central to the cycloadditions is a nucleophilic attack at the C of the nitrile oxide that removes electron density from the P atom of the phosphine facilitating formation of the O-P bond essential for OAT. It would appear, at first sight, that oxidation of basic phosphine ligands and coordinatively unsaturated late transition metal complexes would bear little resemblance. Recent work [12], however has shown that Lewis acid adduct such as that shown in Eq. (11) can be formed.

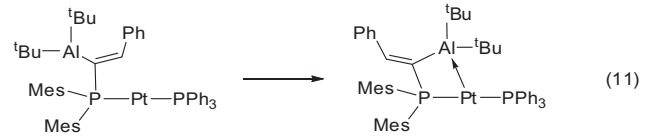
(11)

The ability of Vaska's complex, $IrCl(CO)(PPh_3)_2$, to react with Lewis acids was demonstrated long ago with the formation of its unusual BF_3 adduct [13] and indicates the amphoteric character of electron rich yet coordinatively unsaturated late transition metal compounds.

In the first part of this work, we report the synthesis, structural characterization and preliminary mechanistic studies for the formation of the Pd(II) metallacyclic complex [Pd(IPr)(NCMes)(κ^2-O-N=C-Mes(-N-C(=O)Mes))] by reaction of 3 equivalents of

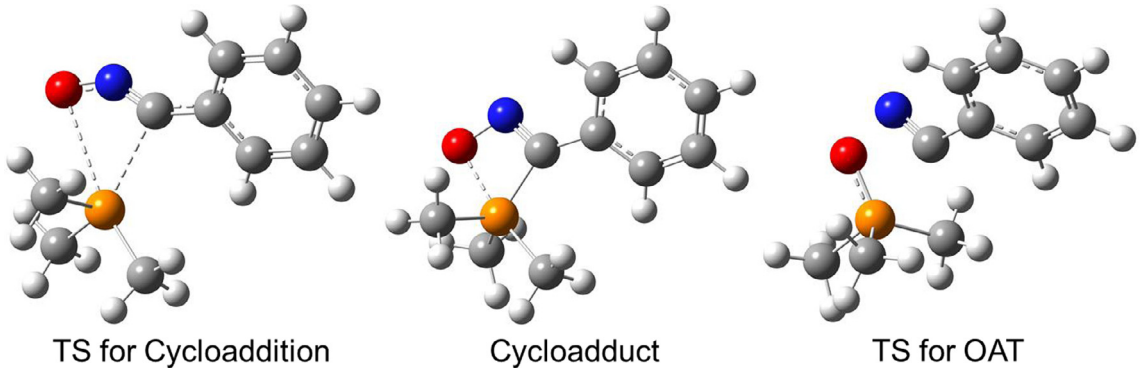

Scheme 1. Selected species in proposed oxidation of PR_3 by MesCNO [11].

MesCNO with [Pd(IPr)(P(p-tolyl)$_3$)] where two OAT reactions from the nitrile oxide to the ligands bound to the metal center occur.

In the second part of this work, we describe studies of addition of ·NO to a metal peroxide complex. The reaction of the peroxide complex to form a N-bonded nitro complex has been known since reaction (12) was reported fifty years ago by Collman [14].

$$L_2Pd(O_2) + 2{\cdot}NO \rightarrow L_2Pd(NO_2)_2 \quad (12)$$

The reaction in Eq. (12), involving two equivalents of nitric oxide with bound molecular oxygen, can be compared to the stepwise reaction (13) for the free gaseous molecules.

$$2 \uparrow NO + \downarrow O_2 \downarrow \rightleftarrows ONOO \downarrow + \uparrow NO \rightleftarrows ONOONO \rightleftarrows \uparrow NO_2 + \downarrow NO_2 \quad (13)$$

Reaction (13) is important in atmospheric chemistry and has been extensively studied. Computational work [15] provides insight into this reaction. The authors are aware of no experimental or computational reports of the mechanism or energetics of reaction (12) in which the metal-based counterpart of reaction (13) occurs. Preliminary synthetic, structural, and computational results are reported in the second part of this contribution in which coordinated oxygen atoms are transferred to rather than from N.

2. Experimental

2.1. General considerations

Unless stated otherwise, all operations were performed in a Vacuum Atmospheres or MBraun glovebox under an atmosphere of purified nitrogen or argon or utilizing standard Schlenk techniques under an Argon atmosphere. Special Schlenk lines were developed that allowed rapid switching from Argon to Oxygen to Argon or other gas atmosphere during the reaction. Solvents were degassed and purified using standard techniques. Anhydrous deuterobenzene or toluene-d_8 were purchased from Aldrich chemical, degassed, and stored over 4 Å molecular sieves in the glove box. Mesityl nitrile oxide was prepared and recrystallized according to the literature [16]. [Pd(IPr)$_2$] and [Pd(IPr)(P(p-tolyl)$_3$)] were prepared as described previously [17]. ^{1}H NMR spectra were recorded on a Bruker Avance-400 spectrometer at room temperature. ^{1}H NMR chemical shifts are reported in parts per million (ppm) with respect to the *protio* impurities referenced at 7.16 ppm for C_6D_6 and 2.09 ppm for toluene-d_8. FTIR spectra were obtained using a Perkin Elmer Spectrum 400 FTIR Spectrometer.

2.2. Reaction of [Pd(IPr)(P(p-tolyl)$_3$)] and MesCNO

In the glove box, 48.5 mg (0.061 mmol) [Pd(IPr)(P(p-tolyl)$_3$)] and 29.5 mg (0.183 mmol) MesCNO (1/3 M ratio) were dissolved in a vial in 2 mL of toluene and left standing for approximately 12 h. During that time, a copious amount of red-orange crystals of high quality precipitated on the walls of the vial. The supernatant liquid was decanted into a Schlenk tube, evacuated to dryness and the solid residue dissolved in C_6D_6. The NMR spectrum showed near quantitative production of O=P(p-tolyl)$_3$, no remaining unreacted MesCNO and only traces of free MesCN. The solid material was isolated in approximately 80% yield. Examination under a microscope showed the crystals to be of high quality as formed. The crystals were suitable for structure determination as described in a later section.

The red-orange complex is sparingly soluble in C_6D_6 and appears to change color in CD_2Cl_2. The ESI-TOF mass spectrum showed a peak at 962.5 assigned to P + 1, at 817.4 assigned to P – NCMes + 1, and at 387.3 assigned to IPr + 1. NMR data of the complex are reported in the Supporting Information.

2.3. Spectroscopic studies of reactions of [Pd(IPr)(P(p-tolyl)$_3$)] and MesCNO

In the glove box a solution was made of 20.8 mg (0.026 mmol) [Pd(IPr)(P(p-tolyl)$_3$)] and 8.1 mg (0.0503 mmol) MesCNO in 3 mL C_6D_6 to form a solution with initial [MesCNO] = 0.0168 M and [Pd(IPr)(P(p-tolyl)$_3$)] = 0.0087 M at a 1.94 to 1 MesCNO/Pd molar ratio. An IR cell and an NMR tube were filled with the solution and its reactivity monitored at 22 °C by IR and 25 °C by NMR. The first FTIR spectrum was run six minutes after mixing the reagents in the glove box and difference spectra were recorded following at regular time intervals. Related reactions were performed on solutions of [Pd(IPr)(P(p-tolyl)$_3$)] and MesCNO in C_6D_6, prepared at 1/1, 1/3 and 1/10 M ratios. Reaction of MesCNO and P(p-tolyl)$_3$ was also investigated using techniques strictly analogous to those reported earlier [11]. In most cases ^{1}H NMR were obtained but ^{31}P NMR spectroscopy was also performed to confirm unequivocally the production of free O=P(p-tolyl)$_3$ as product.

2.4. Reaction of in situ prepared [Pd(IPr)$_2$(η^2-O$_2$)] and ·NO

In the glove box, a Schlenk tube was loaded with 20 mg [Pd(IPr)$_2$] and approximately 10 mL of toluene. The mixture was shaken to completely dissolve the solid yielding an orange colored solution. The Schlenk tube was taken from the glovebox and placed in a −78 °C bath all while under a positive pressure of Argon. The reaction atmosphere was then changed to O_2 producing a dark yellow solution together with a milky white precipitate in keeping with generation of *in situ* [Pd(IPr)$_2$(η^2-O$_2$)] [17]. The oxygen was removed by vacuum and replaced with argon. To this was added 10 mL ·NO by gas tight syringe. The color slowly changed to orange and then to light yellow and then to light yellow-green. The solution was warmed to room temperature under continuous

evacuation to give a yellow-green solid. Extraction with heptane under an argon atmosphere allowed clean separation of the yellow product and filtration of the heptane solution yielded a clear yellow solution which upon cooling to −20 °C in a freezer yielded pure crystals of *trans*-[Pd(IPr)$_2$(NO$_2$)$_2$] (**2**) in approximately 25% yield. These proved suitable for structural study as described below. NMR data are in agreement with the structure of **2** and are provided in the Supporting Information.

2.5. Crystallographic analyses

Red-orange crystals of [Pd(IPr)(NCMes)(κ^2-O-N=C-Mes(-N-C(=O)Mes))] (**1**) were obtained by slow crystallization from the forming solution in toluene as described earlier. Pale yellow crystals of *trans*-[Pd(IPr)$_2$(NO$_2$)$_2$] (**2**) were obtained by slow crystallization from a toluene/heptane mixture in a freezer at −20 °C also for a period of weeks. The data crystal of **2** was mounted onto the end of a thin glass fiber using Paratone-N for data collection at 100 K under N_2. The data crystals of **1** and **2** were glued onto the end of a thin glass fiber. X-ray intensity data were measured by using a Bruker SMART APEX2 CCD-based diffractometer using Mo Kα radiation (λ = 0.71073 Å) [18]. The raw data frames were integrated with the SAINT+ program by using a narrow-frame integration algorithm. Corrections for Lorentz and polarization effects were also applied with SAINT+. An empirical absorption correction based on the multiple measurement of equivalent reflections was applied using the program SADABS [19]. All non-hydrogen atoms were refined with anisotropic displacement parameters. Hydrogen atoms were placed in geometrically idealized positions and included as standard riding atoms during the least-squares refinements. All structures were solved by a combination of direct methods and difference Fourier syntheses, and refined by full-matrix least-squares on F^2, by using the SHELXTL software package [20]. Crystal data, data collection parameters, and results of the analyses are listed in Table 1.

Compounds **1** and **2** crystallized in the monoclinic crystal system. For **2**, the space group $P2_1/c$ was confirmed on the basis of the systematic absences in the data. For **1**, the space groups $P2_1$ and $P2_1/m$ were indicated on the basis of the systematic absences in the data. The structure could only be solved in the former space group.

2.6. Computational methods

All calculations were carried out at the DFT level with an ultrafine grid [21] as implemented in Gaussian 09 suite of programs [22]. Geometry optimizations were performed without any symmetry restrictions using the PBE0 functional [23], the D3(BJ) empirical dispersion correction [24] and the Def2-TZVP [25] basis set for Pd along with the corresponding ECP [26] and the 6-311G(d,p) basis set for the rest of the atoms. We refer to this basis set combination in this work as BSI. All stationary points were optimized by computing analytical energy gradients. The obtained minima were characterized by performing energy second derivatives, confirming them as minima by the absence of negative eigenvalues of the Hessian matrix of the energy. To further refine the energies, single-point calculations were performed using the larger Def2-QZVP [26] and 6-311+G(2d,p) basis set for Pd and the rest of the atoms respectively. We refer to this basis set combination in this work as BSII. In addition, analogous single-point calculations were also carried out with the B3LYP [27] and BP86 [28] density functionals. Computed electronic energies were corrected for zero-point energy, thermal energy and entropic effects to determine ΔH^0(298 K).

3. Results

3.1. Synthesis of Pd(IPr)(NCMes)(κ^2-O-N(=C)-Mes(-N-C(=O)Mes)) (1)

Reaction of MesCNO and [Pd(IPr)(P(p-tolyl)$_3$)] occur in a 3/1 M ratio as shown in Eq. (14) as confirmed by IR and NMR studies.

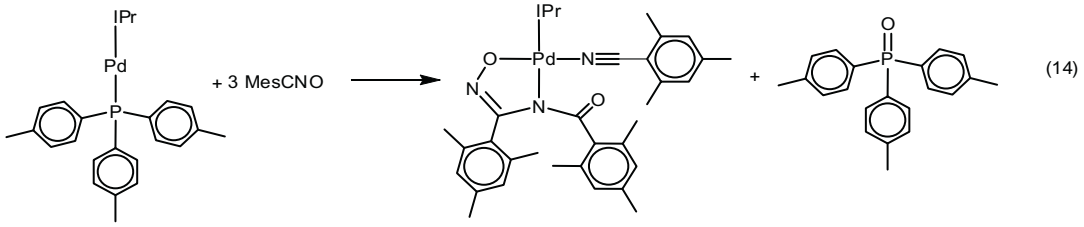

Due to low solubility, the pure crystalline product can be obtained in ≈80% yield. This is best achieved when a slight excess of [Pd(IPr)(P(p-tolyl)$_3$)] is present since excess MesCNO appears to be capable of further reaction with **1** slowly to yield unknown products.

3.2. Mechanistic investigation of reaction of MesCNO and [Pd(IPr)(P(p-tolyl)$_3$)]

A representative plot of IR spectra run to determine the approximate rate law for the reaction is shown in Fig. 1 below. Under these conditions [Pd(IPr)(P(p-tolyl)$_3$)] is present in slight excess. A plot of the difference spectra is shown in Fig. 1 below:

Fig. 1 shows the smooth decrease in concentration of free MesCNO at 1348 cm^{-1} and concurrent increase in free O=P(p-tolyl)$_3$ at 1217 cm^{-1}. The band at 1217 cm^{-1} is assigned to the O=P(p-tolyl)$_3$ stretch in keeping with literature assignments for O=PPh$_3$ [29] and also based on independent study of the reaction of MesCNO and P(p-tolyl)$_3$ under similar conditions [11]. No attempt was made to interpret the other bands that rise and fall during the reaction and are most likely due to differences in free MesCNO versus the metallacyclic complex. The two bands followed are unequivocally assigned to MesCNO and O=P(p-tolyl)$_3$.

Compared to oxidation of the free phosphine by MesCNO, oxidation of the bound phosphine was observed to occur more rapidly

Table 1
Crystallographic data for **1** and **2**.

Compound	**1**	**2**
Empirical formula	$PdO_2N_5C_{57}H_{69}$	$PdO_4N_6C_{54}H_{72}$
Formula weight	962.57	975.57
Crystal system	Monoclinic	Monoclinic
Lattice parameters		
a (Å)	11.3388(7)	21.1672(9)
b (Å)	19.7405(11)	12.5519(6)
c (Å)	12.0599(7)	20.2658(10)
α (deg)	90	90
β (deg)	91.505(1)	97.801(1)
γ (deg)	90	90
V (Å^3)	2698.5(3)	5334.6(4)
Space group	$P2_1$(# 4)	$P2_1/c$(# 14)
Z value	2	4
ρ_{calc} (g/cm^3)	1.185	1.215
μ (Mo K$_\alpha$) (mm^{-1})	0.387	0.395
Temperature (K)	296	296
$2\Theta_{max}$ (°)	50.0	50.0
No. Obs. (I > 2σ(I))	7583	7102
No. Parameters	604	602
Goodness of fit GOF*	1.012	1.070
Max. shift in cycle	0.000	0.008
Residuals*: R1; w*R*2	0.0394; 0.0685	0.0567; 0.1435
Absorption Correction, Max/min	Multi-scan	Multi-scan
	0.7457/0.6692	0.5776/0.7457
Largest peak in Final Diff. Map (e$^-$/Å^3)	0.386	1.094

*$R1 = \Sigma_{hkl}(||F_{obs}| - |F_{calc}||)/\Sigma_{hkl}|F_{obs}|$; $wR2 = [\Sigma_{hkl}w(|F_{obs}| - |F_{calc}|)^2/\Sigma_{hkl}wF_{obs}^2]^{1/2}$, $w = 1/\sigma^2(F_{obs})$; $GOF = [\Sigma_{hkl}w(|F_{obs}| - |F_{calc}|)^2/(n_{data} - n_{vari})]^{1/2}$.

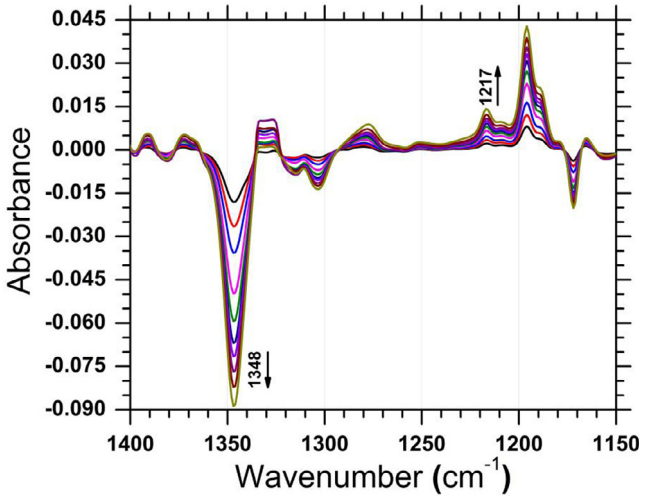

Fig. 1. Difference spectra (observed spectrum – first spectrum) in the region 1400–1150 cm^{-1}.

but to produce only about 1/3 of an equivalent of O=P(p-tolyl)$_3$ in keeping with the stoichiometry of the reaction. Also of note is failure to observe bands in the IR that rise and fall which could be attributed to an intermediate species that accumulates during the reaction. The presence of several isosbestic points in the spectra also point to a clean reaction without accumulation of intermediate complexes.

A plot of the absorbance of MesCNO versus time is shown in Fig. 2 as well as a simulation of absorbance change data based on a second order rate law: d[P]/dt = *k*[Pd(IPr)(P(p-tolyl)$_3$)][MesCNO].

The graph in Fig. 2 is in keeping with this being a second order reaction overall displaying first order dependence on each reactant. That is also in keeping with other qualitative and quantitative studies of the reaction made by IR and NMR of the reaction. Detailed kinetic studies including temperature variation to determine activation parameters were not performed. The primary conclusions regarding the mechanism are qualitative in nature at this time but suggest that any proposed mechanism should be consistent with the following observations:

(i) The rate determining step is approximately first order in both MesCNO and [Pd(IPr)(P(p-tolyl)$_3$)] (ii). The course of the reaction is progressive with the decay of 3 mol of MesCNO paralleling the production of 1 mol of O=P(p-tolyl)$_3$. (iii) There are no indications in the FTIR of bands that rise and fall and no stable intermediate complex is formed at detectable levels during the reaction. (iv) From the beginning, with no induction period there is a smooth buildup of dissociated O=P(p-tolyl)$_3$. There is no spectroscopic evidence of free MesCN or free P(p-tolyl)$_3$ during the reaction.

3.3. Structure of [Pd(IPr)(NCMes)(κ^2-O-N=C-Mes(-N-C(=O)Mes))] (1)

The crystal structure of complex **1** is shown in Fig. 3. Compound **1** is a mononuclear Pd complex that contains a terminal IPr ligand, a terminal NCMes ligand and a κ^2-O-N=C-Mes(-N-C(=O)Mes) group. As seen from the angles around Pd in Fig. 3 caption, the geometry around the Pd atom may be viewed as approximately square planar, and atoms C1-N3-N4-O1 are slightly offset from all lying within a plane. Compound **1** can be considered formally as a Pd(II) complex with a 16-electron configuration where the κ^2-O-N=C-Mes(-N-C(=O)Mes) group serves as a 4 electron donor (2− charge) ligand. The Pd1−N3 distance of 2.020(6) Å to the nitrile group is similar in value to the Pd−N distances in the compounds [Pd(NCPh)$_2$X$_2$] (X = Cl or Br) which range from 1.94(2)–1.99(2) Å [30]. Also the Pd1−N4 distance of 2.050(4) Å to the amide group is close in values to that found in a related cyclopalladium complex, 1.956(2) Å [31]. The cyclic arrangement of atoms with palladium is quite rare and there are only two other reported crystal structures that have that same arrangement of 5 atoms [32].

3.4. Synthesis and structural determination of trans-[Pd(IPr)$_2$(η^1-NO$_2$)$_2$] (2)

As described in the experimental section, reaction of *in situ* prepared [Pd(IPr)$_2$(η^2-O$_2$)] when exposed to ·NO under an argon atmo-

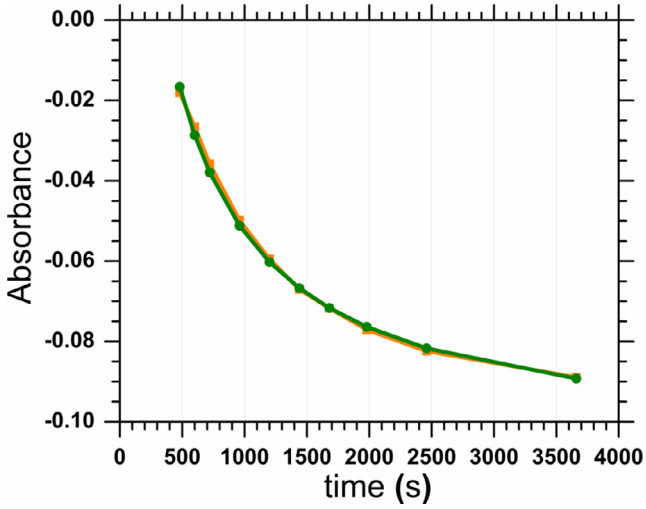

Fig. 2. Plot of [$\Delta A_{1348cm-1}$] versus time (seconds) for reaction of [MesCNO] = 0.0168 M and [Pd(IPr)(P(p-tolyl)$_3$)] = 0.0087 M at a 1.94 to 1 MesCNO/Pd molar ratio in C_6D_6 at 22 °C. The orange curve is actual data and the green curve is the computed data based on an overall second order rate law with first order dependence in each reactant at this unequal concentration of reactants.

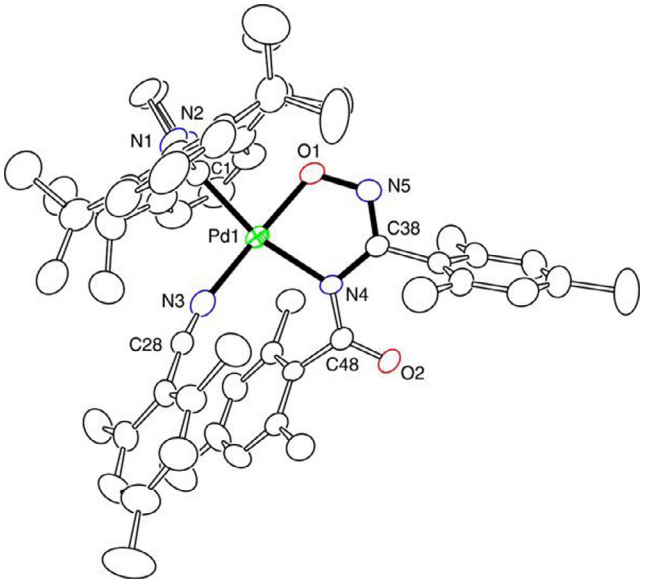

Fig. 3. An ORTEP of the molecular structure of [Pd(IPr)(NCMes)(κ^2-O-N=C-Mes(-N-C(=O)Mes))] (**1**) showing 30% thermal probability ellipsoids. Selected bond distances (in Å) and angles (in °) are as follows: Pd1–O1 = 1.944(3), Pd1–C1 = 2.007(5), Pd1–N3 = 2.020(6), Pd1–N4 = 2.050(4), O1–N5 = 1.386(4), O2–C48 1.236(6), N3–C28 = 1.143(7), N4–C48 = 1.362(6), N4–C38 = 1.402(6), N5–C38 = 1.275(5), O1–Pd1–C1 = 85.07(17), O1–Pd1–N3 = 169.6(3), C1–Pd1–N3 = 96.4 (2), O1–Pd1–N4 = 80.76(14), C1–Pd1–N4 = 165.70(18), N3–Pd1–N4 = 97.93(17).

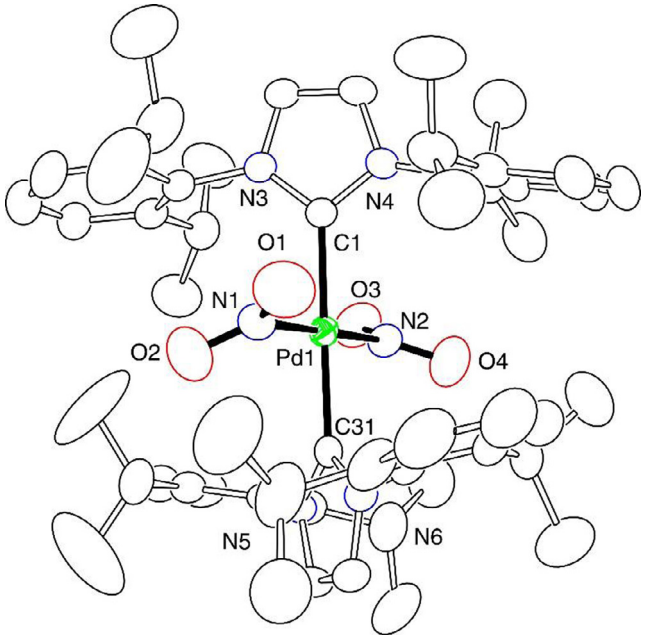

Fig. 4. An ORTEP of the molecular structure of *trans*-[Pd(IPr)$_2$(NO$_2$)$_2$] (**2**) showing 30% thermal probability ellipsoids. Selected bond distances (in Å) and angles (in °) are as follows: Pd1–N2 = 2.024(4), Pd1–N1 = 2.028(4), Pd1–C31 = 2.070(4), Pd1–C1 = 2.075(4), O1–N1 = 1.145(6), O2–N1 = 1.229(6), O3–N2 = 1.193(5), O4–N2 = 1.213(5), N2–Pd1–N1 = 179.49(18), C31–Pd1–C1 = 179.18(15), N2–Pd1–C31 = 90.94(15), N1–Pd1–C31 = 89.05(16), N2–Pd1–C1 = 88.79(16), N1–Pd1–C1 = 91.22(16).

sphere at −78 °C was observed to change from yellow to orange to dark yellow. The light-yellow complex could be extracted using heptane or toluene and recrystallized by cooling in a freezer at −20 °C. The crystal structure of **2** is shown in Fig. 4.

Compound **2** is also a square planar Pd(II) 16 electron complex with the IPr ligands *trans* to each other. The NO_2 ligands are arranged such that all four O atoms do not lie in the same plane. There is indication of some interaction between C–H bonds on the pendant isopropyl groups and N–O bonds of the coordinated nitro groups as shown in Supporting Information. The NO_2 groups are equivalent to each other by C_2 symmetry. The Pd–N and N–O distances are similar to those found in the complex *trans*-[Pd(PPh$_3$)$_2$(NO$_2$)$_2$] [33]. The fact that in *trans*-[Pd(PPh$_3$)$_2$(NO$_2$)$_2$] all four O atoms lie in the same plane, while in (**2**) they do may be due to the C–H−−O bonding interactions. A figure showing these interactions is provided in Supporting Information. Insufficient data are available at this time to assess the significance of these interactions.

3.5. Computational results

Density functional theory (DFT) was employed to provide insights into the reaction energetics of formation of *in situ* prepared [Pd(IPr)$_2$(η^2-O$_2$)] and 2 ·NO. The optimized structure of *trans*-[Pd(IPr)$_2$(η^1-NO$_2$)$_2$] **2** was found to be in excellent agreement with the X-ray structural determination. In order to gain insight about reaction energetics, computations were done using a truncated model of the Pd complex, [Pd(IMe)$_2$], where the 2,6-diisopropylphenyl substituents on the nitrogen atoms of the IPr carbenes coordinated to the Pd center are replaced by methyl groups. The truncated models [Pd(IMe)$_2$], [Pd(IMe)$_2$(η^2-O$_2$)] and *trans*-[Pd(IMe)$_2$(NO$_2$)$_2$] were computed (see SI for more details) and enthalpies of reaction computed as shown in the thermochemical cycle in Scheme 2.

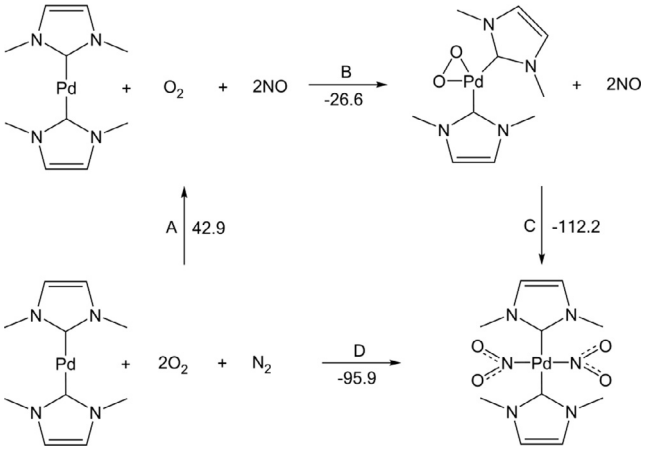

Scheme 2. Enthalpies of reaction (kcal/mol) relevant to formation of *trans*-[Pd(IMe)$_2$(NO$_2$)$_2$] computed at the BP86-D3(BJ)/BSII//PBE0-D3(BJ)/BSI level (see computational details section).

4. Discussion

The goal of this work was to study reactions involving the making and breaking of N-O bonds in reactions with low valent Pd complexes. That is part of a long-range goal aimed at understanding catalytic processes involving transition metal catalyzed OAT reactions of N_xO_y compounds. The first part of this work involved our initial studies of the reaction between MesCNO and [Pd(IPr)(P(p-tolyl$_3$)$_2$)]. This work builds upon earlier mechanistic and thermochemical studies of OAT reactions utilizing MesCNO as a potent

agent for transfer of a single oxygen atom to metals and also non-metals [4,11]. It was hoped that direct evidence for formation of an intermediate "L_nPdO" complex would emerge, either by detection of an intermediate or in isolation of a stable dimeric complex of the form $[Pd(IPr)(L)(\mu\text{-}O)]_2$ in which L = MesCN or P(p-tolyl)$_3$ formed by dissociation of one ligand to form a stable oxo bridged square planar structure. No such direct evidence was found. Instead, relatively clean formation of **1** occurred. The stoichiometry of the product forming reaction involves assembly of three equivalents of MesCNO with one equivalent of [Pd(IPr)(P(p-tolyl)$_3$)].

The following overall processes must occur during this reaction: (a) One mole of MesCNO serves to oxidize the PR_3 ligand. The MesCN produced in this reaction coordinates to the metal; (b) A second mole of MesCNO undergoes OAT to form the C=O bond found in the product; (c) The remaining MesCNO ligand does a cycloaddition reaction yielding product. A general mechanism for these steps is shown in Scheme 3:

The order of these steps does not have to occur as shown, but it seems most reasonable to the authors that the rate determining step which is first order in both MesCNO and Pd(IPr)(P(p-tolyl)$_3$)] would be OAT to produce O=P(p-tolyl)$_3$. The phosphine oxide produced should be a weakly bound token "ligand" and readily undergo rapid ligand substitution. Dissociation of O=P(p-tolyl$_3$) and its replacement by MesCN or MesCNO would be expected to allow for facile rearrangements in subsequent steps due to reduction in steric hindrance. This is in keeping with our initial kinetic studies showing a rate limiting second order reaction step between reactants with no buildup of intermediates.

The driving force for the proposed first reaction would be strong. Replacement of the weak MesCN-O bond (BDE = 54 kcal/mol) [2] by the much stronger O=P(p-tolyl)$_3$ bond (BDE = 138 kcal/mol) [11] which should be exothermic by more than 80 kcal/mol. The second major step proposed in Scheme 3 is OAT from MesCNO to a C atom to form ultimately a benzamido complex similar to that shown in the mechanism by Bergman [10] in Eq. (10). The driving force for this reaction is again replacement of the weak MesCN-O bond by the relatively strong C=O bond formed as well as oxidation of Pd from formally Pd(0) to Pd(II). Preliminary computational results attest to the thermochemical feasibility of this reaction [34].

The final step of the sequence would then involve a cycloaddition of MesCNO at the highly basic imido N atom of the benzamido complex at the C atom of the MesCNO-this would lead to the final product by establishment of a Pd-O bond to the O of the incoming MesCNO while cleaving the bond to the coordinated ketone yielding product. This proposal was also motivated by the mechanism proposed for O=ZrCp$*_2$ (Eq. 10). Steric strain, as well as a negative formal charge on the highly basic N of the benzamido complex should provide the driving force for the nucleophillic attack at the C atom of the third mole of MesCNO yielding **1**. While the authors view this as a reasonable overall mechanism that is consistent with observed experimental results and also literature reports by other groups, it is not established. Details of the precise formulation of the complexes are not shown, however, these three steps appear key.

The potential complexity of these steps is shown in Scheme 4 which illustrates several possible mechanisms for the initial reaction of MesCNO and [Pd(IPr)(P(p-tolyl)$_3$)].

The first step shown is formation of *cis*-$[ML_1L_2(\kappa^2\text{-RCNO})]$ in a rapid pre-equilibrium step. This would involve $[ML_1L_2]$ attacking the C atom of RCNO and also coordinating through the O atom in a manner resembling that proposed for PR_3 oxidation as shown in Scheme 1. This is in keeping with the recent work [12] highlighting the Lewis base reactivity shown in Eq. (11). It is also in accord with failure to observe reaction of $[Pd(IPr)_2]$ and MesCNO under similar conditions since adoption of a *cis* geometry for the *bis* IPr system results in significant steric as is the case [17] for $[M(IPr)_2(\eta^2\text{-}O_2)]$.

Formation of low steady state concentrations of *cis*-$[ML_1L_2(\kappa^2\text{-RCNO})]$ is believed to occur prior to rate determining OAT to either the Pd center or to the P(p-tolyl)$_3$ ligand in our system (L_1 in Scheme 4) by one of two routes in the probable rate determining step for the overall reaction. This can occur by two potential pathways that would be kinetically indistinguishable. The first would be formation of a transition state oxo complex $[ML_1L_2(RCN)(O)]$ which then undergoes OAT as shown in reactions 1 followed by reaction 2 in Scheme 4. This complex resembles intermediates proposed by Gould [6] and Bohle [7], and discussed earlier (see reactions 5 and 6). However, a pathway in which the κ^2-RCNO ligand attacks first the Pd-PR_3 $\sigma*$ bond and then forms a P-O bond cannot be ruled out and is shown in the single concerted step reaction (1,2) Concerted.

In addition to OAT to L_1, two additional key reactions of the postulated "$[ML_1L_2(RCN)(O)]$" complex are also shown in Scheme 4. The K_{eq} dimer step shows the well-established formation of the dimeric bridging oxo structure which is well documented [35]. One reason for the successful isolation of the Milstein Pt(IV)-O complex in Eq. (3) is that the bulky ancillary pincer ligand serves to inhibit dimerization of this type. Recently, we have reported the role of reaction sterics on the monomer/dimer bridging hydride reaction for bulky triorganotin platinates with ancillary NHC ligands [36]. Varying the NHC ligand was shown to play a key role in influencing this reaction.

The final key reaction of "$L_1L_2(RCN)M\text{-}O$" shown is oxygen migration to the C atom of the coordinated nitrile. This is shown in reaction 3 followed by reaction 4 which results in formation of a benzamido complex. This resembles the mechanism proposed by Bergman and coworkers [10] and shown in Eq. (10). Not shown in the scheme (for clarity) is that the step 3 concerted followed by 4 can also lead to the benzamido complex. The authors could only find one crystallographically determined true benzamido complex in the Cambridge database [10c]. The proposed benzamido complex in Scheme 4 fits the requirement that OAT has occurred to the C atom, and the basic N should be capable of attack at the C of the third MesCNO to yield the final product as shown. Precedent for this type of reactivity is shown in the work of Kukushkin [8].

The second part of this work involves OAT to rather than from N. In spite of the report fifty years ago by Collman [14], to the authors' knowledge, the mechanism for conversion of a bound peroxide by two moles of ·NO to two moles of ·NO_2 has not been

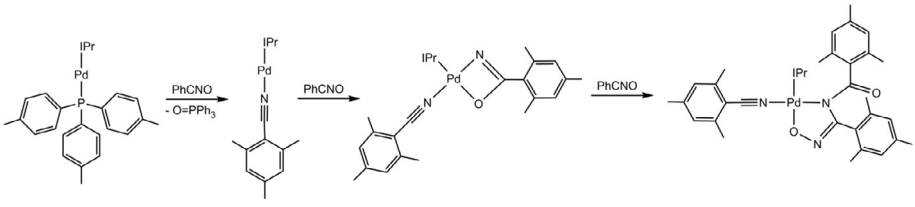

Scheme 3. Major steps proposed for the formation of **1**.

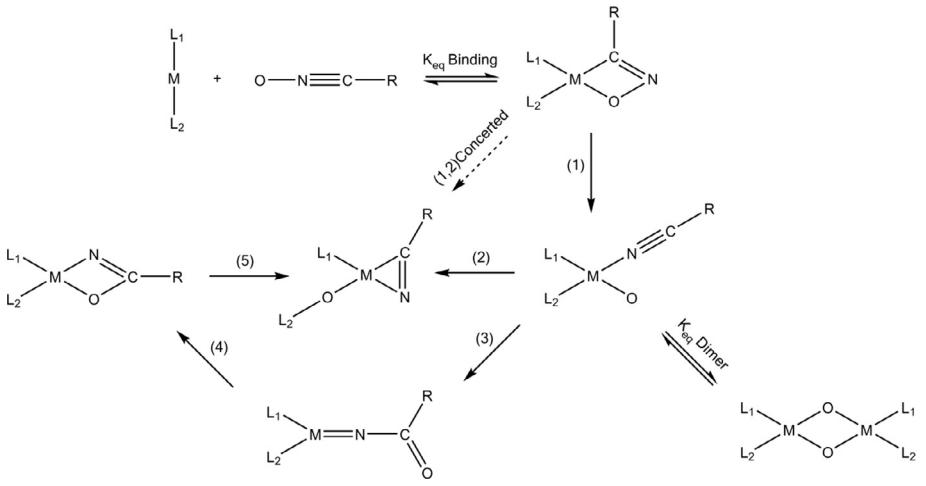

Scheme 4. Possible first steps in reaction of L_1ML_2 and RCNO (L_1 = PR_3 or other oxidizable ligand, L_2 = NHC or other less readily oxidized ligand, M = Pd, Pt.

elucidated. As with the formation of **1**, the formation of **2** presents a number of challenges in mechanistic inorganic chemistry.

Four potential mechanisms appear reasonable for this reaction. The first, and one that can be ruled out would involve loss of coordinated O_2 which then reacts with 2 ·NO as shown in reaction (13) to yield 2·NO_2 as is well known. Two equivalents of ·NO_2 so formed would be expected to undergo rapid coordination as shown in Eq. (15)

$$[Pd(IPr)_2] + 2{\cdot}NO_2 \rightarrow \textit{trans}\text{-}[Pd(IPr)_2(NO_2)_2] \quad (15)$$

The complex $[Pd(IPr)_2(\eta^2\text{-}O_2)]$ has a weak Pd-O_2 bond [17] and readily dissociate O_2. However, preliminary studies [34] appear to indicate that reaction with 2 ·NO occurs at an overall rate faster at low temperatures than O_2 loss. In addition, $[Pd(IMes)_2(\eta^2\text{-}O_2)]$ which requires temperatures [37] on the order of ≈60 °C to lose O_2, readily adds ·NO at ambient temperatures. For that reason, dissociation of bound O_2 from $[Pd(L)_2(\eta^2\text{-}O_2)]$ followed by reaction of free O_2 with 2 ·NO is not viewed as a likely mechanism. The remaining three mechanisms all involve attack of ·NO on the Pd of $[Pd(L)_2(\eta^2\text{-}O_2)]$, or on the O of either $[Pd(L)_2(\eta^2\text{-}O_2)]$ or $[Pd(L)_2(\eta^1\text{-}O_2)]$. Kinetic studies of this reaction for a range of low valent peroxide complexes are planned.

The most surprising aspect of this second project was the computed reaction energetics shown in Scheme 2. In particular reaction D that forms the bound *bis*-nitro complex from N_2 and O_2 is computed to be highly favorable from a thermodynamic point of view. Utilizing these data and tabulated literature values [2], the reactions shown Eqs. (16) and (17) can be compared:

$$[Pd(IMe)_2] + 2{\cdot}NO_2 \rightarrow \textit{trans}\text{-}[Pd(IMe)_2(NO_2)_2] \quad \Delta H^0 = -112\ \text{kcal/mol} \quad (16)$$

$$H_2(g) + 2{\cdot}NO_2 \rightarrow 2HNO_2(g) \quad \Delta H^0 = -52\ \text{kcal/mol} \quad (17)$$

The computed energy of reaction (16) is 60 kcal/mol more exothermic than (17). Attempts to directly measure by solution calorimetric methods the enthalpy of formation of **2** by reaction (16) are planned to test the accuracy of our computed data.

5. Conclusion

This work reports the surprisingly efficient reaction of three moles of MesCNO with one mole of [Pd(IPr)(Pd(p-tolyl)$_3$)] to form [Pd(IPr)(NCMes)(κ^2-O-N=C-Mes(-N-C(=O)Mes))]. During the reaction two of the three N-O bonds of the reacting nitrile oxides undergo OAT. A possible mechanism is proposed based on qualitative and semi-quantitative studies. The possibility of formation of unstable intermediate complexes containing L_nPd-O bonds is mentioned as a possibility. The premise that such bonds should be weak remains unchallenged but the active participation of such species and even possibly their eventual isolation remains possible. MesCNO itself is unstable with respect to MesCN and ½ O_2 from a thermodynamic perspective. The mechanism outlined is one of many possible and incorporates plausible driving forces for the individual steps. Due to the weakness of the N-O bond broken in MesCNO as well as the weakness of any temporary Pd-O bond formed as an intermediate a number of possible routes exist until the weak N-O bond is converted to a strong P=O or C=O bond in the product.

The reaction of $[Pd](IPr)_2(\eta^2\text{-}O_2)]$ with two equivalents of ·NO to form *trans*-$[Pd(IPr)_2(NO_2)_2]$ resembles reaction (12) reported by Collman of the PPh_3 analog reported nearly fifty years ago [14]. Reaction (13) for the O_2(g) and 2 ·NO(g) to make 2 ·NO_2(g) occurs with an enthalpy of activation near 0 kcal/mol and a nearly constant rate over a 600 °C temperature range [15]. Detailed study of reaction of a range of Pd and Pt peroxo complexes and ·NO is underway in our laboratory to allow comparison of free versus bound dioxygen reactivity with nitric oxide. The computational result that formation of **2** from N_2 and $2O_2$ is thermochemically favorable provides incentive for investigation of chemical/electrochemical catalytic oxidation of N_2 itself as first suggested almost a century ago by Lewis and Randall [38].

Acknowledgments

This article is dedicated to Professor Luis Echegoyen. Support of this work by the National Science Foundation (Grant No. CHE-1300206 to BC), the Brazilian National Council for Scientific and Technological Development (CNPq process 213876/2014-0), the ERC (FUNCAT to SPN), CTQ2016-80600-P (MINECO, Spain to MT) is gratefully acknowledged.

Appendix A. Supplementary data

Supplementary data associated with this article can be found, in the online version, at http://dx.doi.org/10.1016/j.ica.2017.05.069.

References

[1] (a) E.N. Martín, M. Altable, S. Filippone, A.M. Domenech, R.M. Álvarez, M. Suarez, M.E.P. Brzezinska, O. Lukoyanova, L. Echegoyen, J. Org. Chem. 72 (2007) 3840;
(b) M. Alvaro, P. Atienzar, P. de la Cruz, J.L. Delgado, V. Troiani, H. Garcia, F. Langa, A. Palkar, L. Echegoyen, J. Am. Chem. Soc. 128 (2006) 6626.
[2] (a) Y.R. Luo, Handbook of Bond Dissociation Energies in Organic Compounds, CRC Press, Boca Raton, 2003;
(b) http://webbook.nist.gov/chemistry/form-ser.html.
[3] W. Beck, M. Keubler, E. Leidl, U. Nagel, M. Schaal, S. Cenini, P. Del Buttero, E. Licandro, S. Maiorana, A.C. Villa, J. Chem. Soc. Chem. Commun. 10 (1981) 446.
[4] T. Palluccio, E.V.R. Akimova, X. Cai, S. Majumdar, M. Temprado, J.S. Silvia, A.F. Cozzolino, D. Tofan, C.C. Cummins, B. Captain, C.D. Hoff, J. Am. Chem. Soc. 135 (2013) 11357.
[5] (a) H.B. Gray, C.R. Hare, Inorg. Chem. 1 (1962) 363;
(b) J.R. Winkler, H.B. Gray, Struct. Bonding (Berlin) 142 (2011) 17.
[6] M.A. Andrews, G.L. Gould, E.J. Voss, Inorg. Chem. 35 (1996) 5740.
[7] N. Arulsamy, D. Scott Bohle, J.A. Imonigie, S. Levine, Angew. Chem. Int. Ed. 41 (2002) 2371.
[8] (a) D.S. Bolotin, N.A. Bokach, A.S. Kritchenkov, M. Haukka, V.Y. Kukushkin, Inorg. Chem. 52 (2013) 6378;
(b) M.L. Kuznetsov, A.A. Nazarov, L.V. Kozlova, V.Y. Kukushkin, J. Org. Chem. 72 (2007) 4475;
(c) G. Wagner, A.J.L. Pombeiro, V.Y. Kukushkin, J. Am. Chem. Soc. 122 (2000) 3106;
(d) V.Y. Kukushkin, A.J.L. Pombeiro, Chem. Rev. 102 (2002) 1771;
(e) A.S. Kritchenkov, N.A. Bokach, G.L. Starova, V.Y. Kukushkin, Inorg. Chem. 51 (2012) 11971.
[9] (a) E. Poverenov, I. Efremenko, A.I. Frenkel, Y.B. David, J.L.J.W. Shimon, G. Leitus, L. Konstantinovski, J.M.L. Martin, D. Milstein, Nature 455 (2008) 1093;
(b) I. Efremenko, E. Poverenov, J.M.L. Martin, D. Milstein, J. Am. Chem. Soc. 132 (2010) 14886.
[10] (a) M.J. Carney, Patrick J. Walsh, G. Robert, J. Bergman, Robert G. Bergman, Am. Chem. Soc. 112 (1990) 6426;
(b) Michael J. Carney, P.J. Walsh, F.J. Hollander, R.G. Bergman, Organometallics 11 (1992) 761;
(c) T.T. Nguyen, G.D. Kortman, K.L. Hull, Organometallics 35 (2016) 1713.
[11] X. Cai, S. Majumdar, G.C. Fortman, L.M. Frutos, M. Temprado, C.R. Clough, C.C. Cummins, M.E. Germain, T. Palluccio, E.V.R. Akimova, B. Captain, C.D. Hoff, Inorg. Chem. 20 (2011) 9620.
[12] M. Devillard, R. Declercq, E. Nicolas, A.W. Ehlers, J. Backs, N. Saffon-Merceron, G. Bouhadir, J.C. Slootweg, W. Uhl, D. Bourissou, J. Am. Chem. Soc. 138 (2016) 4917.
[13] R.N. Scott, D.F. Shriver, L. Vaska, J. Am. Chem. Soc. 90 (1968) 1080.
[14] (a) J.P. Collman, M. Kubota, J.V. Hosking, J. Am. Chem. Soc. 89 (1967) 4809;
(b) J.P. Collman, Acc. Chem. Res. 1 (1968) 136.
[15] (a) H. Gunaydin, K.N. Houk, J. Am. Chem. Soc. 130 (2008) 10036;
(b) A.B. McCoy, M.K. Sprague, M. Okumura, J. Phys. Chem. A 114 (2010) 1324;
(c) Y. Zhao, K.N. Houk, P.L. Olson, J. Phys. Chem. A 108 (2004) 5864;
(d) S. Goldstein, G. Czapski, J. Lind, G. Merenyi, Chem. Res. Toxicol. 14 (2001) 657.
[16] (a) M.V. Barybin, P.L. Diaconescu, C.C. Cummins, Inorg. Chem. 40 (2001) 2892;
(b) C. Grundmann, J.M. Dean, J. Org. Chem. 30 (1965) 2809.
[17] (a) X. Cai, S. Majumdar, G.C. Fortman, C.S.J. Cazin, A.M.Z. Slawin, C. Lhermitte, R. Prabhakar, M.E. Germain, T. Palluccio, S.P. Nolan, E.V. Rybak-Akimova, M. Temprado, B. Captain, C.D. Hoff, J. Am. Chem. Soc. 133 (2011) 1290;
(b) T. Pallucio, X. Cai, S. Majumdar, L. F. Serafim, N. C. Tomson, K. Wieghardt, C. S. J. Cazin, S. P. Nolan, E. V. Rybak-Akimova, M. A. Fernández-González, M. Temprado, B. Captain, C. D. Hoff, Manuscript in preparation.
[18] Apex2 Version 2.2-0 SAINT+ Version 7.46A; Bruker Anal. X-ray Syst. Inc., Madison, Wisconsin, USA, 2007.
[19] Sheldrick, G. M. SHELXTL Version 6.1; Bruker Anal. X-ray Syst. Inc., Madison, Wisconsin, USA, 2000.
[20] G.M. Sheldrick, Acta Cryst. C71 (2015) 3.
[21] S.E. Wheeler, K.N. Houk, J. Chem. Theory Comput. 6 (2010) 395.
[22] M.J. Frisch, G.W. Trucks, H.B. Schlegel, G.E. Scuseria, M.A. Robb, J.R. Cheeseman, G. Scalmani, V. Barone, B. Mennucci, G.A. Petersson, H. Nakatsuji, M. Caricato, X. Li, H.P. Hratchian, A.F. Izmaylov, J. Bloino, G. Zheng, J.L. Sonnenberg, M. Hada, M. Ehara, K. Toyota, R. Fukuda, J. Hasegawa, M. Ishida, T. Nakajima, Y. Honda, O. Kitao, H. Nakai, T. Vreven, J.A. Montgomery Jr., J.E. Peralta, F. Ogliaro, M. Bearpark, J.J. Heyd, E. Brothers, K.N. Kudin, V.N. Staroverov, T. Keith, R. Kobayashi, J. Normand, K. Raghavachari, A. Rendell, J.C. Burant, S.S. Iyengar, J. Tomasi, M. Cossi, N. Rega, J.M. Millam, M. Klene, J.E. Knox, J.B. Cross, V. Bakken, C. Adamo, J. Jaramillo, R. Gomperts, R.E. Stratmann, O. Yazyev, A.J. Austin, R. Cammi, C. Pomelli, J.W. Ochterski, R.L. Martin, K. Morokuma, V.G. Zakrzewski, G.A. Voth, P. Salvador, J.J. Dannenberg, S. Dapprich, A.D. Daniels, O. Farkas, J.B. Foresman, J.V. Ortiz, J. Cioslowski, D.J. Fox, Gaussian 09, revision D.01, Gaussian Inc., Wallingford CT, 2013.
[23] C. Adamo, V. Barone, J. Chem. Phys. 110 (1999) 6158.
[24] S. Grimme, S. Ehrlich, L. Goerigk, J. Comput. Chem. 32 (2011) 1456.
[25] F. Weigend, R. Ahlrichs, Phys. Chem. Chem. Phys. 7 (2005) 3297.
[26] D. Andrae, U. Haeussermann, M. Dolg, H. Stoll, H. Preuss, Theor. Chim. Acta. 77 (1990) 123.
[27] (a) A.D. Becke, J. Chem. Phys. 98 (1993) 5648;
(b) C. Lee, W. Yang, R.G. Parr, Phys. Rev. B 37 (1988) 785.
[28] (a) A.D. Becke, Phys. Rev. A 38 (1988) 3098;
(b) J.P. Perdew, Phys. Rev. B 33 (1986) 8822.
[29] I. Reva, L. Lapinski, M.J. Nowak, Chem. Phys. Lett. 467 (2008) 97.
[30] M.M. Olmstead, P.P. Wei, A.S. Ginwalla, A.L. Balch, Inorg. Chem. 39 (2000) 4555.
[31] S.K. Zhang, X.Y. Yang, X.M. Zhao, P.X. Li, J.L. Niu, M.P. Song, Organometallics 34 (2015) 4331.
[32] (a) S. Herold, F. Boccini, Inorg. Chem. 45 (2006) 6933;
(b) W.-W. Han, W.J. Long, New Cryst. Struct. 229 (2014) 87.
[33] (a) A. Abellan-Lopez, M.-T. Chicote, D. Bautista, J. Vincente Dalton Trans. 43 (2014) 592;
(b) M.R. Warren, S.K. Brayshaw, L.E. Hatcher, A.L. Johnson, S. Schiffers, A.J. Warren, S.J. Teat, J.E. Warren, C.H. Woodall, P.R. Raithby, Dalton Trans. 41 (2012) 13173.
[34] M. Temprado, B. Captain, C. C. Cazin, S. P. Nolan. L. F. Serafim, C. D. Hoff, work in progress.
[35] (a) C. Kerpal, D.J. Harding, A.C. Hermes, G. Meijer, S.R. Mackenzie, A. Fielicke, J. Phys. Chem. A 113 (2013) 1233;
(b) S.M. Lang, I. Fleischer, T.M. Bernhardt, R.N. Barnett, U. Landman, J. Phys. Chem. A 118 (2014) 8572.
[36] (a) A. Koppaka, B. Captain, Inorg. Chem. 55 (2016) 2679;
(b) A. Koppaka, V. Yempally, L. Zhu, G. Fortman, M. Temprado, C.D. Hoff, B. Captain, Inorg. Chem. 55 (2016) 307.
[37] M.M. Konnick, I.A. Guzei, S.S. Stahl, J. Am. Chem. Soc. 126 (2004) 10212.
[38] G.N. Lewis, M. Randall, Thermodynamics-The Free Energy of Chemical Substances, McGraw Hill, New York, 1923.